ELSEVIER

SPECTROCHIMICA ACTA PART B

Spectrochimica Acta Part B 54 (1999) 1335–1350

www.elsevier.nl/locate/sab

Comparison between a radio-frequency and direct current glow discharge in argon by a hybrid Monte Carlo–fluid model for electrons, argon ions and fast argon atoms

Annemie Bogaerts[a,*], Renaat Gijbels[a], Wim Goedheer[b]

[a] *Department of Chemistry, University of Antwerp, Universiteitsplein 1, B-2610 Wilrijk-Antwerp, Belgium*
[b] *FOM-Institute for Plasmaphysics 'Rijnhuizen', P.O. Box 1207, 3430 BE Nieuwegein, The Netherlands*

Received 10 February 1999; accepted 28 May 1999

Abstract

A hybrid Monte Carlo–fluid model has been developed for the electrons, argon ions and fast argon atoms in an argon glow discharge, either operated in the dc mode or the capacitively coupled rf mode. Typical working conditions for rf GD-OES are considered, i.e. approximately 6 torr argon gas pressure and approximately 10 W power. Typical results of the model, like the potential distributions, densities, fluxes and ionization rates, will be presented and compared between the two operation modes. It will be demonstrated that the rf discharge yields more efficient ionization than the dc discharge, and hence the rf discharge requires lower voltages to obtain the same amount of power, which is in good correspondence to experimental observations.

Keywords: Glow discharge; rf; dc; Argon; Modeling; Monte Carlo model; Fluid model; Hybrid model; Plasma

1. Introduction

Glow discharge plasmas are being used in various application fields, e.g. materials processing in the semiconductor industry, the flat plasma display panel technology, the laser and light industry. Moreover, they find also application in analytical chemistry, for the trace analysis in solid materials [1,2]. In the latter application, the solid sample is used as the cathode or rf-powered electrode of an argon glow discharge (in a dc and capacitively coupled rf discharge, respectively), and is being sputtered by plasma species. The sputtered,

* Corresponding author. Tel.: +32-3820-2364; fax: +32-3820-2376.
E-mail address: bogaerts@uia.ua.ac.be (A. Bogaerts)

0584-8547/99/$ - see front matter
PII: S0584-8547(99)00080-4

analytically important atoms can be ionized or excited in the glow discharge plasma. The ionization collisions create ions of the cathode material, which can be measured with a mass spectrometer, giving rise to glow discharge mass spectrometry (GDMS). The excitation collisions, followed by decay to lower levels, yield photons characteristic for the material to be analyzed, which can be detected with optical emission spectrometry (GD-OES).

For the analysis of metals, a dc glow discharge is very convenient, due to its simplicity and stable operation conditions. However, non-conducting materials cannot directly be analyzed with a dc glow discharge, because they would be charged up when used as the cathode, due to positive ion bombardment, thereby preventing the plasma ions from further bombarding and sputtering. However, this problem is overcome by applying an rf voltage between the electrodes, so that the positive charge accumulation due to positive ion bombardment will be neutralized by an equal amount of negative charge accumulated by electron bombardment during a part of the rf-cycle.

In the literature, a number of groups have made comparisons between glow discharges in the dc and rf mode, by looking at the analytical characteristics. Marcus and coworkers [3] have found that an rf discharge generally yields shorter stabilization times and less variation over extended periods of operation. Moreover, the signal-to-background ratios in the optical emission spectra appear to be higher in an rf-discharge. On the other hand, the sputtering rates and the raw intensities seem to be lower in the rf-plasma [3]. The same trend was found by Pereiro and coworkers [4] in a similar source geometry (the Marcus-cell). They found that the rf-discharge needs approximately 4–8 W power to reach the same amount of sputtering as a dc-discharge at 1 W, but they suggest that this can be explained since the rf-power measured at the generator does not necessarily enter for 100% into the discharge. Kim and coworkers [5] studied a jet-boosted glow discharge in the dc and rf modes, and they found that the dc mode yielded three times more sputtering than the rf discharge at comparable power levels. The rf-mode, on the other hand, showed lower detection limits than the dc-mode. The emission intensities were comparable for some lines, but they were higher or lower for others [5]. Hoffmann and his group demonstrated that for their equipment (Grimm-source) the sputtering and excitation were rather similar in both the dc and rf modes [6,7]. Moreover, they measured lower voltages (rf amplitude and dc bias voltage) in the rf mode, which suggests that this mode yields more efficient ionization [8]. Harrison and coworkers [9,10] found that the rf-mode needed 10 times higher power levels to reach the same amount of sputtering at similar pressures. Moreover, the rf-mode required more power for comparable ion intensities in the mass spectrum [9]. However, the authors suggest also that this is attributed to the power losses in the rf-mode. Payling observed similar analytical characteristics in both the dc and rf discharges [11]. Finally, Wagatsuma and Suzuki found that 'equivalent discharge conditions', yielding similar analytical characteristics (erosion rates and emission intensities) could be obtained in both operation modes; the equivalent condition for the dc mode at 500 V and 30 mA appeared to be 100 W in the rf-discharge at the same pressure, hence again a higher power [12], which is, however, probably again due to power losses in the rf-mode.

In general, it appears from all these experimental observations that the rf discharge requires somewhat more power to yield the same amount of sputtering, but this is probably due to power losses in the rf-discharge. The reported emission intensities and the analytical characteristics look more or less similar. In order to draw conclusions about fundamental differences between the dc and rf modes, it is, however, very important to make comparisons at exactly specified conditions (e.g. constant power, constant pressure or constant emission intensities). Indeed, different results can be obtained depending on which conditions are kept constant. It is not always clear from the experimental data which conditions were held the same, probably because various operating conditions cannot easily be measured (e.g. the exact gas pressure in both dc and rf modes, and

the power, voltages and currents in the rf-mode). Moreover, analytical GD-users are mainly interested in having similar analytical characteristics in both modes which they wish to compare, and therefore, they often prefer to make comparisons at e.g. the same erosion rates; in this way they do not have to deal with accurate measurements of the discharge conditions as such [13].

In order to understand and compare the main features of both discharge modes, we have developed a 3D hybrid Monte Carlo–fluid model for the electrons, argon ions and fast argon atoms in a dc [14–16] and an rf glow discharge [17–19]. In the present paper, the modeling results for the dc and rf discharge in argon will be compared at similar discharge conditions, typically used for GD-OES. In Section 2, a brief description of the model will be given. The results will be discussed and the two operation modes compared in Section 3. Finally, a conclusion will be presented in Section 4.

2. Description of the model

2.1. Discharge conditions

The glow discharge cell under investigation is a simple cylinder, 2 cm in length and 0.25 cm in diameter. The cathode or rf-powered electrode is placed at one end of the cylinder, whereas the other cell walls are grounded. Due to the large difference in size of the rf-powered and grounded electrodes, a large dc bias voltage is expected to arise in the case of the rf-discharge, which is beneficial for sputtering. The typical working conditions, used as input in the models are 13.56 MHz rf-frequency, 5.775 torr argon gas pressure and approximately 10-W power. More exactly, the incoming power of 10 W was used as input in the rf model. In the dc model, the discharge voltage is standardly given as input, whereas the electrical current, and hence also the power, are obtained as output (see below). Hence, we had to find out, by 'intelligent guessing', which voltage yielded a power of approximately 10 W. Moreover, we take $T = 1000$ K, which seems realistic for the power value under consideration [20].

These discharge conditions and cell geometry were suggested by Hoffmann [8]. He found out that these values of power and pressure (more exactly 10.2 W rf power and 11 W dc power) yielded very similar analytical results in both the dc and rf mode. Moreover, he has measured the voltages for these values of power and pressure, both in the rf and dc mode, in a Grimm-type glow discharge with 2.5 mm anode diameter. The rf amplitude and dc bias voltage in the rf-mode were measured to be 764 V and -627 V, and the dc voltage in the dc-mode was found to be 1100 V [8]. These measured values will be used as a check for our calculation results. The cell geometry in our model is only an approximation of a real Grimm-type geometry (but with the same anode diameter), in order not to further complicate the calculations.

2.2. Monte Carlo models

A three-dimensional Monte Carlo model is developed for the electrons in the entire discharge [14,15,17,19], and another one for the argon ions and fast argon atoms (created from the argon ions by charge transfer and momentum transfer collisions) in the sheath in front of the rf-electrode or cathode [16,18].

Briefly, the Monte Carlo models follow all particles (i.e. electrons, argon ions or fast argon atoms) during successive time-steps. The trajectory of these particles is calculated with Newton's laws, the probability for collision is calculated from the collision cross-sections and the density of the target particles, and compared to a random number. If the collision probability is lower than the random number, no collision occurs, and the next particle is followed during that time-step. If the collision probability is higher than the random number, a collision does take place, and the kind of collision is then determined by another random number, based on the partial collision probabilities. Collisions taken into account in the electron Monte Carlo model are elastic collisions, electron impact ionization and excitation, and electron–electron Coulomb collisions. The cross-sections for these collisions as a function of the electron energies are adopted from refs [21,22],

and the formulas of these cross-sections are presented also in ref. [17]. A detailed description of the electron–electron Coulomb collisions, a process which was not incorporated before in our dc models [14,15], is also given in ref. [17]. In the Monte Carlo model for argon ions and fast argon atoms, charge transfer and momentum transfer collisions, as well as fast argon ion and atom impact ionization and excitation were considered. The cross-sections for these processes were obtained from refs [23,24]. When the new energy and direction after the collision are determined, the next particle is followed in the same way. This procedure is repeated during many time-steps and for many particles.

It should be mentioned that in the electron Monte Carlo model only 'fast electrons' are followed. Indeed, once the electrons arrive in the bulk plasma (negative glow) and have energies lower than the threshold for inelastic collisions (ionization and excitation), they are not really important as fast electrons. Their only role is to carry the electrical current and to provide negative space charge. It would take a very long calculation time to keep following all these electrons with the Monte Carlo method. Therefore, they are transferred to the slow electron group, which is treated in a fluid model.

2.3. Fluid model

The fluid model for electrons and argon ions throughout the discharge [14,15,17,19] has been developed in two dimensions. Indeed, due to the cylindrical symmetry of the discharge cell, the three dimensions could be reduced to two dimensions (axial and radial direction). Input for this fluid model are the creation rates of ions and electrons, which are obtained from the Monte Carlo model [i.e. electron, fast argon ion and atom impact ionization rate and/or slow electron transfer rate (see below)]. The equations in this model are the ion and electron continuity equations and flux equations based on diffusion and on migration in the electric field. In the rf model, also the electron energy balance equation is incorporated, to calculate the slow electron mean energy, which is necessary to compute the ionization in the fluid model. Indeed, in the rf model, the slow electrons can be heated again by the fluctuating electric field and they can produce some extra ionization, as will be explained below. These continuity, flux and energy balance equations are coupled to Poisson's equation, to obtain a self-consistent electric field distribution. It should be mentioned that the argon ions in the rf case cannot follow the rapidly fluctuating electric field, and hence they feel only an effective electric field, which is nearly equal to the time-averaged electric field. The outputs of the fluid model are, among others, the electric field and the ion flux, both as a function of position and time in the rf-cycle (for the rf-case). They are used as inputs in the electron, argon ion and fast argon atom Monte Carlo models, to determine the trajectory of these particles, and also the electron flux leaving the rf-electrode (or cathode) due to secondary electron emission, and the argon ion flux entering the sheath (obtained from the ion flux at the rf-electrode (cathode) and at the sheath–plasma interface, respectively).

Only secondary electron emission due to argon ion bombardment is considered, with a secondary electron emission coefficient equal to 0.083 (which is typical for a copper electrode [25]). When a clean electrode surface is assumed (as is justified here, because the rf electrode/cathode will continuously be sputter-cleaned) secondary electron emission due to argon atom bombardment can be neglected at the moderate argon atom energies under consideration here (i.e. calculated to be around 10 eV [18,26]). Indeed, for clean surfaces, the argon atom induced secondary electron emission coefficient is very low for atom energies below 700 eV, and starts to increase only for higher atom energies [27].

2.4. Differences between the rf and dc models

In this way, the Monte Carlo and fluid models are coupled, and they are solved iteratively until convergence is reached. Details about the Monte Carlo and fluid models for both discharge modes can be found in refs [14–19] and will not be

repeated here. However, we will briefly address the main differences in the models for the dc and rf discharge:

(1) As mentioned before, the Monte Carlo model considers only the fast electrons, and the slow electrons are treated in the fluid model. There is, however, an important difference between the dc and rf models. Indeed, in the dc mode, when the electrons are slowed down in the negative glow, they remain slow. However, in the rf mode, the slow electrons can be heated again by the fluctuating electric field [both in the moving rf-sheath (which is called 'wave-riding') but also in the bulk plasma where the electric field can be quite high around $\omega t = \pi/2$, see below]. These heated electrons can then produce again ionization, which is called 'α-ionization', in contrast to 'γ-ionization' which is produced by the electrons emitted from the rf electrode and the subsequent electrons formed in the plasma with sufficient energy to cause further ionization. More details about these two ionization mechanisms can be found (e.g. [19,28–30]). It is clear that in the dc mode, only γ-ionization plays a role. This phenomenon of α-ionization is the reason of the more efficient ionization in the rf mode compared to the dc mode (see later). The α-ionization is calculated in the fluid model, based on an empirical formula for the ionization rate coefficient as a function of the electron mean energy. The latter is, therefore, also calculated explicitly in the rf fluid model with an electron energy balance equation. More details about the electron energy balance equation and the description of α-ionization in the rf fluid model are given by Bogaerts et al. [17,19], respectively.

(2) Another major difference between the two cases is the question of time-dependence. Indeed, the dc model runs under steady state conditions, and although the electrons, argon ions and fast argon atoms are followed in the Monte Carlo models during successive time-steps, the input and output data are independent of time. The Monte Carlo calculations are therefore stopped when: (i) the electrons are absorbed at the walls or transferred to the slow electron group; (ii) the argon ions are neutralized at the walls; and (iii) the fast argon atoms are again slowed down until thermal energy due to collisions. In the rf Monte Carlo simulation, however, the particles are really followed as a function of time, in the time-varying electric field. The Monte Carlo calculations are run during a number of rf-cycles until periodic steady state is reached, i.e. when the effects of all previous rf-cycles on the last rf-cycle (where the sampling of output data takes place) are taken into account. In practice, this happened already at the second rf-cycle for the electron Monte Carlo model [17]. For the argon ion and fast argon atom Monte Carlo model, approximately 25–30 rf-cycles had to be followed before periodic steady state was reached, due to their higher mass and hence lower velocity [18]. It may appear strange that the electrons have to be followed only for two rf cycles whereas the argon ions and atoms needed to be followed for approximately 25–30 cycles, because as long as heavy particles are in a transient regime, the electron behavior will also change and therefore vary from cycle to cycle until all particles come to periodic steady state. However, the electron and ion/atom Monte Carlo models are calculated separately from each other, and the output data of both Monte Carlo models, as a function of time, are only collected during the last rf cycle. In this way, the electrons do not need to be followed for the same number of rf-cycles as the heavy particles.

(3) As mentioned in the introduction, there is also a difference in the input and output data of both models. Indeed, the dc model uses the discharge voltage as input value, beside the gas pressure and temperature, and calculates the electrical current self-consistently, i.e. as the sum of the fluxes of the charged plasma species. In the rf model, however, the incoming power is used as input value, because this is more readily available from a practical point of view. The rf and dc bias voltages are then calculated self-consistently. Indeed, the rf voltage is adapted so that the power calculated based on the product of voltage and current, i.e. $P = (1/T)\int_0^{2\pi} V(t)\cdot I(t)\mathrm{d}t$, is equal to the fixed input power. Similarly, the dc bias voltage is adapted after each rf-cycle by the condition that the ion and electron fluxes at the rf-powered electrode must be equal to each other

when integrated over the entire rf-cycle, as is imposed by the capacitive rf coupling [17].

Finally, it should be mentioned that, in order to be sure about the present comparison, we have also run our rf model under 'dc conditions', i.e. constant potential between the two electrodes. In this case, the dc model is also run until steady state is reached and the results do not vary in time anymore. Moreover, the power was then also used as input value, and the voltage was adapted in the same way as in the rf model (see above). We found that both the 'pure dc' model and the 'rf model run for dc conditions' yielded exactly the same results. This was used to ensure that possible differences between the dc and rf modes are not due to differences in the model approximations, but are really due to differences in operation of both modes.

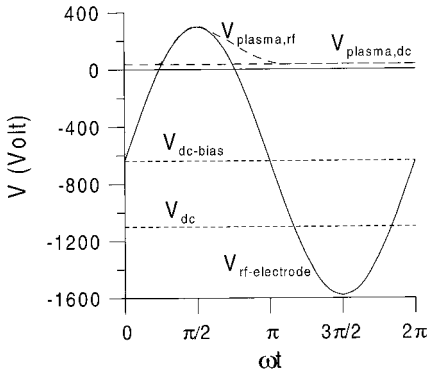

Fig. 1. Electrical potential at the rf-electrode ($V_{\text{rf-electrode}}$; solid line), dc bias voltage ($V_{\text{dc-bias}}$), and plasma potential ($V_{\text{plasma,rf}}$) in the rf discharge. Also shown are the operating voltage (V_{dc}) and plasma potential ($V_{\text{plasma,dc}}$) in the dc discharge ($p = 5.775$ torr, $P = 10.2$ W rf and 10.45 W dc).

3. Results and discussion

3.1. Electrical potential

Fig. 1 shows the potential at the rf-electrode as a function of time in the rf-cycle, at 5.775 torr pressure, 1000 K gas temperature and 10.2 W incoming power. It has a sinusoidal profile, with a negative offset of -640 V (i.e. the dc bias voltage). The amplitude of the sine wave is 937 V. The measured rf amplitude and dc bias voltages, for exactly the same conditions, were 764 V rf amplitude and -627 V dc bias [8] (see before). Hence, the calculated dc bias voltage is in good agreement with the experimental value, but the calculated rf amplitude is somewhat too high. This may be due to approximations in the model (e.g. fluid approximation in the calculation of the electron mean energy and ionization rate coefficient, and a simplified cell geometry). However, the calculated rf amplitude is already in the correct order of magnitude, and what is more important, the calculated rf voltages are lower than the calculated dc voltage (see below), as is also found experimentally [8]. It should be mentioned that with the first version of our rf model (when the description of α-ionization was not yet incorporated in the fluid model [17], see later), the opposite result was obtained, and the calculated rf voltages appeared to be higher than the calculated dc voltage. This indicated that the ionization was, at that time, not correctly described in our rf model. Hence, at present we are already quite satisfied with the correct tendency in the calculated results. Moreover, the voltage waveform presented in Fig. 1 is also qualitatively very similar to the measured waveform presented in Hoffmann et al. [7]. It should be mentioned, however, that most rf generators do not yield a perfectly sinusoidal waveform, due to the superposition of higher order waveforms. The rf generator used to produce the experimental data was, however, sinusoidal within 10%. In future work, the effect of distortions on the sine-wave might be investigated.

It appears that the calculated potential at the rf-electrode is negative during most of the rf-cycle; it is only positive around $\omega t = \pi/2$. Also illustrated in the figure is the plasma potential, indicated by $V_{\text{plasma,rf}}$ (dashed line). It is always positive, but oscillates between a minimum and a maximum value, and is strongly anharmonic. It is nearly constant (around 35 V) when the voltage at the rf-electrode is negative, and increases to approximately 300 V (i.e. more or less equal to the voltage at the rf-electrode) at $\omega t = \pi/2$.

For the same conditions of gas pressure and temperature, the measured voltage in the dc-case

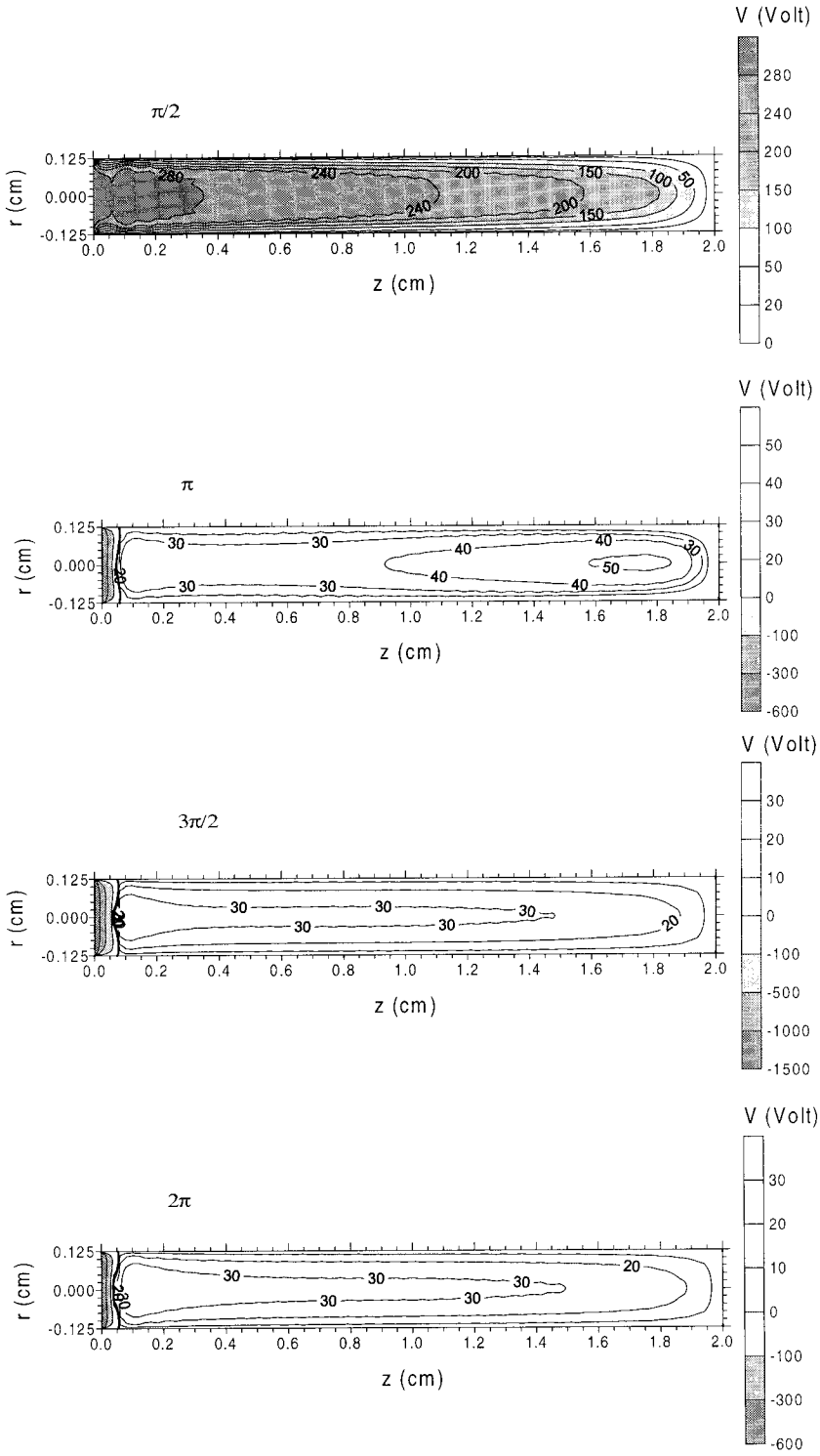

Fig. 2. Two-dimensional potential distribution in the rf-discharge, throughout the discharge region at four times in the rf-cycle ($p = 5.775$ torr, $P = 10.2$ W).

(i.e. 1100 V) resulted in a calculated current of 9.5 mA, hence in a calculated power of 10.45 W, which is in excellent agreement with the measured power value of 11 W [8]. This dc voltage is also indicated in the figure. Hence, it is clear that in the dc mode a higher voltage than the dc bias voltage (which can be considered as the equivalent to the voltage in the dc mode) is required to yield more or less the same power value as in the rf-mode. This indicates that the latter mode yields more efficient ionization, due to the heating of slow electrons in the fluctuating electric field, and the subsequent possibility of α-ionization by these electrons. This will be discussed in more detail further in this paper.

Although the voltage in the dc-mode was found to be higher than the dc bias voltage in the rf-mode, the dc plasma potential was calculated to be 35 V (see Fig. 1, $V_{\text{plasma,dc}}$), which is exactly equal to the rf plasma potential (at least when the voltage at the rf-electrode is negative).

Fig. 2 shows the calculated two-dimensional potential distributions at four times in the rf-cycle. At $\omega t = \pi/2$, the potential is very positive (almost 300 V) at the rf-electrode. It decreases only slowly to zero at the grounded electrode walls. At the other three times in the rf-cycle shown here, the potential is extremely negative at the rf-electrode, as followed also from Fig. 1. It is approximately -640 V at $\omega t = \pi = 2\pi$ (i.e. equal to the dc bias voltage) and almost -1600 V at $\omega t = 3\pi/2$ (i.e. equal to the sum of the dc bias voltage and the rf amplitude). The potential crosses zero at less than 1 mm from the rf-electrode, and reaches a positive value in the bulk plasma (i.e. approximately 50 V at $\omega t = \pi$, and approximately 35 V at $\omega t = 3\pi/2$ and $\omega t = 2\pi$; called the plasma potential). It returns to zero at the grounded electrode walls. This two-dimensional potential distribution at $\omega t = \pi$, $3\pi/2$ and 2π resembles strongly a typical dc potential distribution, as is shown in Fig. 3. Indeed, the potential is also very negative at the cathode (i.e. -1100 V for the dc-case under consideration). It crosses also the zero-line at less than 1 mm from the cathode, and reaches also a positive value of 35 V in the negative glow (the plasma potential), before it returns to zero at the anode walls.

The position where the potential crosses the zero-line is defined here as the interface between rf-sheath and bulk plasma (in the rf-case), or between the cathode dark space and negative glow (dc-case). In the rf-discharge, the rf-sheath varies in thickness, as is illustrated in Fig. 4. It varies between 0 at $\omega t = \pi/2$ (i.e. there is no rf-sheath) and approximately 0.6 mm at $\omega t = 3\pi/2$ (i.e. when the largest potential drop of almost 1600 V takes place). The thickness of the cathode dark space in the dc discharge, which is also depicted in Fig. 4, is approximately 0.8 mm for the discharge conditions under investigation. This value is slightly higher than in the rf case. Indeed, the dc mode yields a higher voltage and hence lower current (see below) for the same

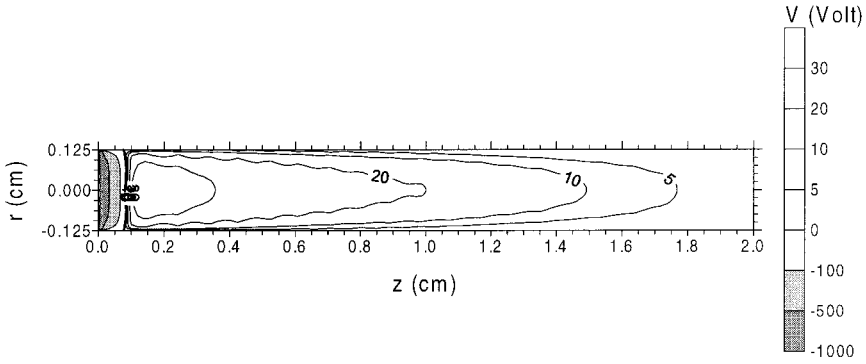

Fig. 3. Two-dimensional potential distribution in the dc-discharge, throughout the discharge region ($p = 5.775$ torr, $P = 10.45$ W, $V = 1100$ V).

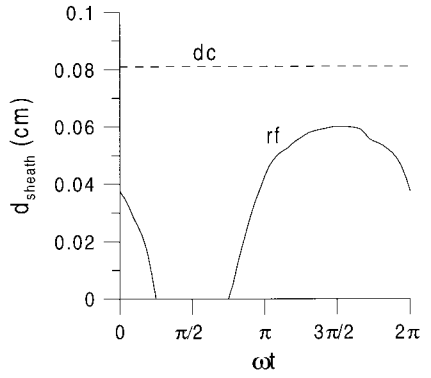

Fig. 4. Thickness of the rf-sheath as a function of time in the rf-cycle, and thickness of the cathode dark space in the dc-discharge ($p = 5.775$ torr, $P = 10.2$ W rf and 10.45 W dc).

power value as the rf mode, and following the empirical formula of Aston [31]:

$$d_{\text{sheath}} = \frac{A}{p} + \frac{B}{I^{1/2}}$$

the sheath thickness, at constant pressure, is known to increase with decreasing current (see also Bogaerts and Gijbels [16]).

3.2. Electrical current

Fig. 5 shows the electrical currents in the rf-discharge calculated at the rf electrode, as a function of time in the rf-cycle. The total electrical current is symbolized with the thick solid line. It is negative during the most part of the rf-cycle (approx. -7 to -20 mA) and strongly positive around $\omega t = \pi/2$ (values till 100 mA). Integrated over the entire rf-period, the total electrical current flowing through the rf-discharge is zero, as is imposed by the capacitive rf-coupling. This total electrical current is the sum of the ion and electron currents, and the displacement current, all taken at the rf electrode. The latter current arises from the moving of the rf-sheath; indeed, this gives a change in the accumulated positive charge and hence, it results in a current, since $I = \mathrm{d}q/\mathrm{d}t$. From Fig. 5 follows, however, that this displacement current, J_D, is negligible at the discharge conditions under investigation, since the rf-sheath indeed did not change very much in thickness (only till maximum 0.6 mm; see Fig. 4). At lower gas pressures and lower dc bias voltages, the displacement current is (in the rf-sheath) generally of comparable magnitude to or even higher than the ion or electron currents [32,33]. This illustrates again that at the high gas pressure and dc bias voltage under consideration here, the rf-discharge very much resembles a dc discharge.

Therefore, at the discharge conditions under study, the ion and electron currents at the rf electrode determine the total electrical current. The ion current (thin solid line) is negative during the entire rf-period, which means that the ions are always directed towards the rf-electrode and that sputtering of the electrode material occurs during the entire rf-cycle, in spite of the fact that the potential at the rf-electrode is positive around $\omega t = \pi/2$. The electron current at the rf electrode (long dashed line) is zero during most of the rf-cycle, except around $\omega t = \pi/2$, where it becomes extremely negative (i.e. directed towards the rf electrode), due to the low mass and hence, the high mobility of the electrons. This 'boost' of electron current is necessary to compensate for the positive charge accumulation, as is imposed by the capacitive rf-coupling.

Also plotted in Fig. 5 is the ion flux at the cathode, in the dc discharge (shorter dashed line), which is equal to -8.8 mA. Most of the time, it is

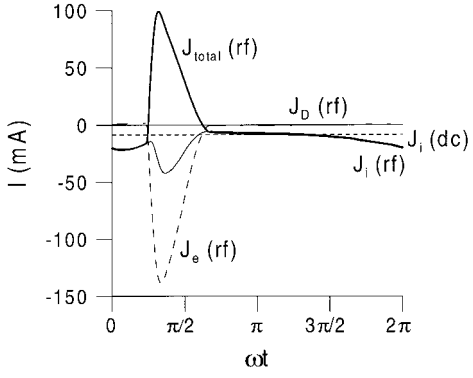

Fig. 5. Total electrical current at the rf-electrode [J_{total}(rf)], and contributions of the ion current [J_i(rf)], electron current [J_e(rf)] and displacement current [J_D(rf)], also at the rf-electrode, as a function of time in the rf-cycle. Also shown is the ion current in the dc-discharge at the cathode [J_i(dc)] ($p = 5.775$ torr, $P = 10.2$ W rf and 10.45 W dc).

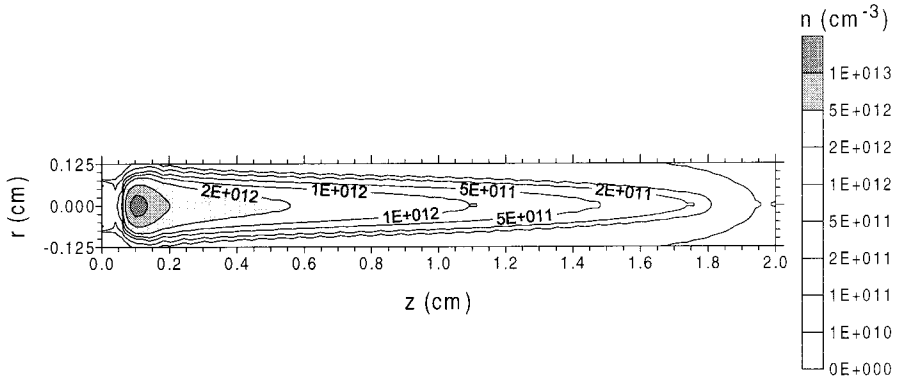

Fig. 6. Two-dimensional argon ion density profile in the rf-discharge, throughout the discharge region at $\omega t = \pi/2$ ($p = 5.775$ torr, $P = 10.2$ W). The results at the other times in the rf-cycle are comparable.

slightly lower than in the rf-discharge (up to a factor of 2), which is attributed to the somewhat lower current in the dc discharge, for the same power (see above).

3.3. Positive ion and electron densities

Fig. 6 shows the two-dimensional argon ion density at $\omega t = \pi/2$. It is more or less constant during the entire rf-cycle since the argon ions cannot follow the rapidly fluctuating electric field due to their high mass and low mobility. The argon ion density is low and more or less constant in the rf-sheath (approx. 3×10^{11} cm^{-3}), and increases to a maximum value of approximately 10^{13} cm^{-3} around 1 mm from the rf-electrode. Then, it decreases again to lower values at the cell walls. The electron density is nearly equal to the argon ion density in the plasma bulk, giving rise to more or less charge neutrality and hence a low electric field. The same is true for the rf-sheath at $\omega t = \pi/2$, where the electric field is again low (or the potential nearly constant, see Fig. 2; strictly speaking, there is no rf-sheath at this time). However, at the other times in the rf-cycle, the electron density returns to zero in the rf-sheath, resulting in a positive space charge

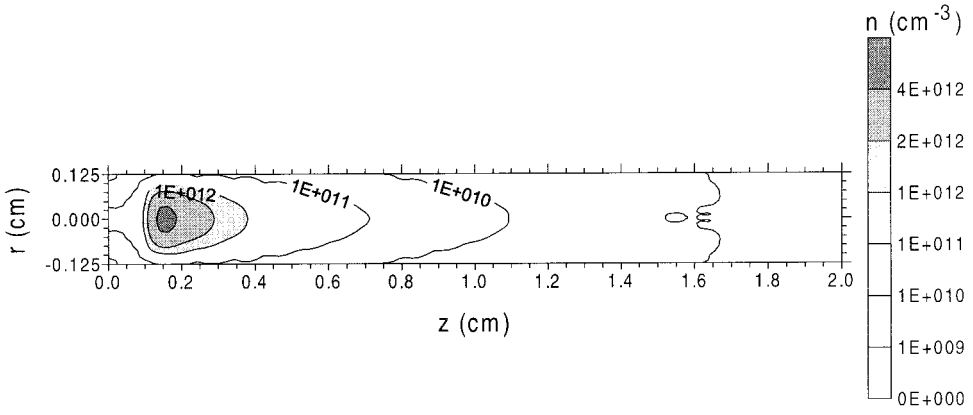

Fig. 7. Two-dimensional argon ion density profile in the dc-discharge, throughout the discharge region ($p = 5.775$ torr, $P = 10.45$ W, $V = 1100$ V).

and hence a high electric field (or large potential drop, see Fig. 2).

The two-dimensional argon ion (and electron) density profiles are in very good qualitative agreement with the ion and electron density distributions in the dc discharge, as follows from Fig. 7. The dc argon ion density profile is also low and rather constant (approx. 10^{11} cm^{-3}) in the cathode dark space, and reaches a maximum at approximately 1.5 mm from the cathode. The absolute value of the maximum is, however, a factor of two smaller (i.e. approx. 4×10^{12} cm^{-3}), which is again the result of the somewhat less efficient ionization and lower current in the dc discharge.

3.4. Ionization rates

The electron impact ionization rate of argon throughout the discharge, calculated with the electron Monte Carlo model, at four times in the rf-cycle, is illustrated in Fig. 8. At $\omega t = \pi/2$, the ionization is rather low, with a maximum at the rf electrode, because the electrons in the Monte Carlo model have rather low energies at this time (see also Bogaerts et al. [17]) and cannot produce efficient ionization. At the other times in the rf-period, the ionization rate is clearly higher and it is characterized by a maximum around 1 mm. Indeed, in the beginning of the bulk plasma, the electrons are not directed by a strong electric field and can scatter back and forth, giving rise to a longer residence time in the plasma and hence more chance for ionization. The same situation occurs in the dc discharge (see Fig. 9): the maximum is found around 1 mm from the cathode, which is the beginning of the negative glow. The absolute value of the maximum is somewhat higher than the results in Fig. 8, at $\omega t = \pi$, $3\pi/2$ and 2π. However, the ionization rates shown in Fig. 8 apply only to γ-ionization, i.e. ionization due to electrons emitted from the rf electrode and electrons formed by ionization with sufficient energy to cause some more ionization. This ionization mechanism is simulated in the Monte Carlo model. However, as mentioned before, the electrons which are slowed down in the bulk plasma can also be heated again by the fluctuating electric field (either in the moving rf-sheath or in the bulk plasma where, at $\omega t = \pi/2$, a moderate electric field is present; see the potential drop in Fig. 2 at $\pi/2$). Subsequently, these electrons can produce ionization, which is called α-ionization. This ionization mechanism is described in our fluid model.

Fig. 10 presents the α-ionization rates, calculated with the fluid model, at four times in the rf-cycle. At $\omega t = \pi/2$, the α-ionization rate is very high, both adjacent to the rf-electrode, and in the bulk plasma. Indeed, the latter region is characterized by a moderate electric field, which is just sufficient to heat the electrons to energies suitable for ionization (see also Bogaerts et al. [19] for more details). At the other times in the rf-cycle, α-ionization occurs at the end of the rf-sheath. Indeed, around $\omega t = \pi/2$, the electrons are drawn towards the rf-electrode (see the negative electron current in Fig. 5). A fraction of these electrons can really reach the rf-electrode; the remaining fraction will be overtaken by the moving rf-sheath at the times later than $\omega t = \pi/2$, and they will be accelerated again away from the rf-electrode by the strong electric field which again dominates now in the rf-sheath. These electrons produce again some ionization at the end of the rf-sheath, as is shown in Fig. 10. When comparing Figs. 8 and 10, it is clear that α-ionization due to slow electrons which become again heated is generally higher than γ-ionization. This is most pronounced at $\omega t = \pi/2$. Therefore, averaged over the entire rf-cycle, the ionization in the rf-mode will be clearly higher than in the dc-mode, due to the extra mechanism of α-ionization.

The electron impact ionization rate of argon in the rf-discharge (i.e. the sum of α and γ ionization), integrated over the entire discharge region, is plotted in Fig. 11 as a function of time in the rf-cycle (upper figure, solid line). It reaches a pronounced maximum around $\omega t = \pi/2$, due to the distinct contribution of α-ionization (see also Fig. 10, i.e. a high value maintained over a long distance). The electron impact ionization rate per second, calculated for the dc mode, integrated over the entire discharge region, is also plotted in this figure (dashed line). It is approximately 7×10^{16} s^{-1}. This value is comparable to the electron

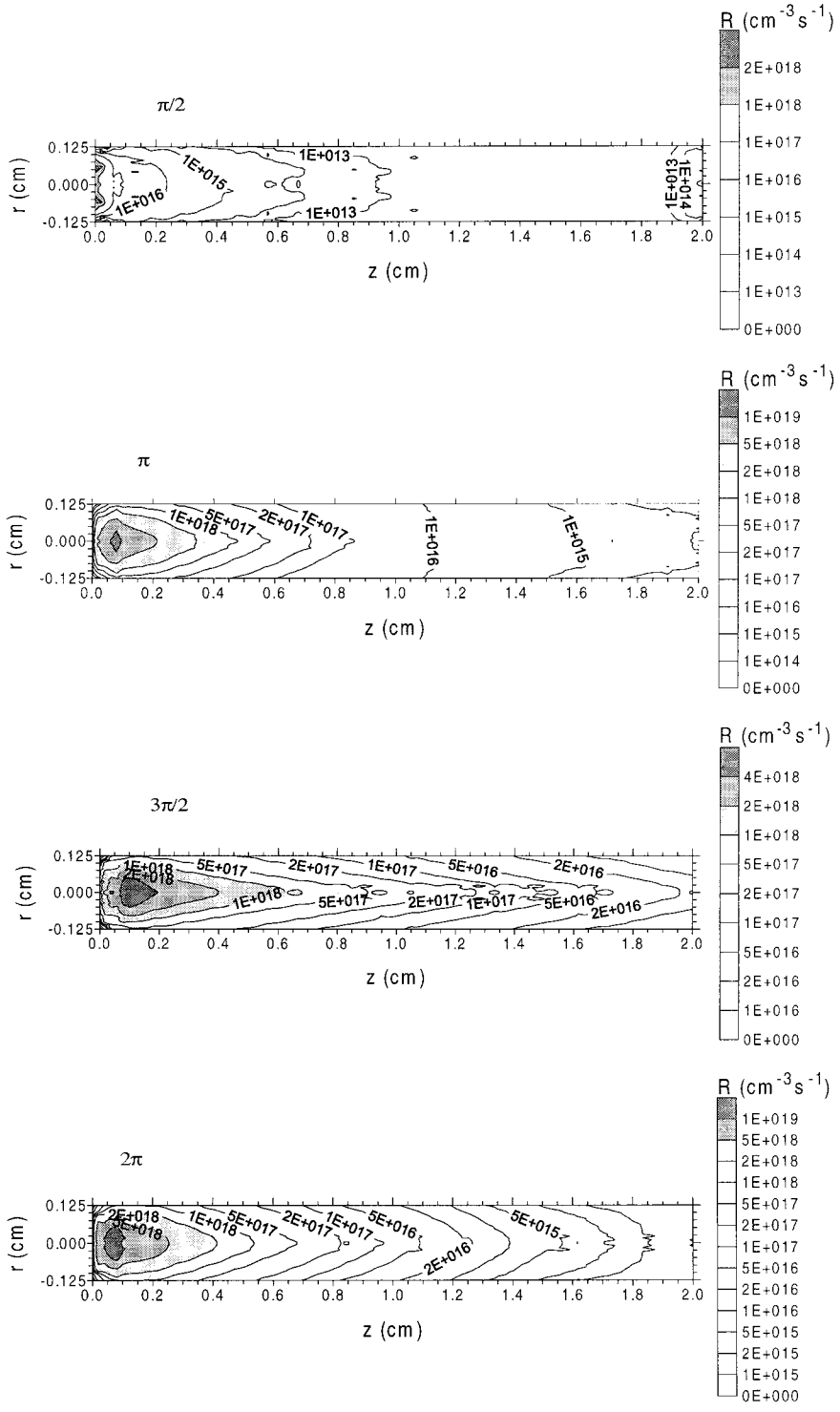

Fig. 8. Two-dimensional electron impact γ-ionization rate of argon in the rf-discharge, throughout the discharge region at four times in the rf-cycle, calculated with the Monte Carlo method ($p = 5.775$ torr, $P = 10.2$ W).

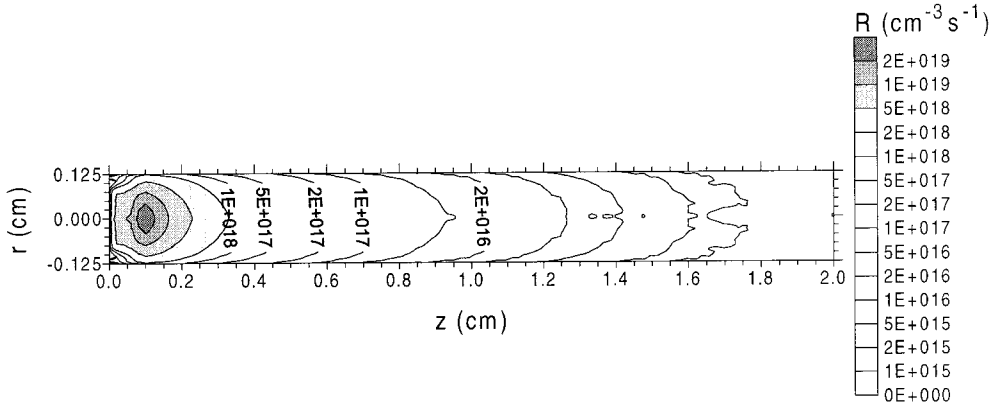

Fig. 9. Two-dimensional electron impact ionization rate of argon in the dc-discharge, throughout the discharge region ($p = 5.775$ torr, $P = 10.45$ W, $V = 1100$ V).

impact ionization rate in the rf-case, at times other than $\pi/2$. However, due to the pronounced peak of the rf ionization rate around $\omega t = \pi/2$, the overall ionization in the dc case is clearly lower.

Beside the electrons, also fast argon ions and fast argon atoms can yield ionization of the argon gas. The cross-sections of fast argon ion and atom impact ionization clearly increase with increasing ion and atom energy, and are only important for energies higher than a few 100 eV [23]. Hence, these processes occur only in the rf-sheath (or cathode dark space) close to the rf-electrode (or cathode), where the electric field is high and the ions and atoms can reach high energies. The fast argon ion and atom impact ionization rates in the rf-discharge, integrated over the entire discharge region, are also plotted in Fig. 11 as a function of time in the rf-cycle (lower part of the figure, solid lines). Because these processes play only a role close to the rf-electrode, the total ionization produced by these processes is lower than for electron impact ionization (i.e. a factor of 10–50 for the atoms, and a factor of 30–150 for the ions). Moreover, these processes have a maximum contribution around $\omega t = 0 = 2\pi$, where the argon ions and fast argon atoms reach the highest energy (see the results obtained in Bogaerts and Gijbels [18]). Also shown in this lower figure are the fast argon ion and atom impact ionization rates calculated for the dc case, integrated over the discharge region. It appears that the dc values are very close to the time-averaged values of the rf ionization rates. Hence, fast argon ion and atom impact ionization seem to occur more or less equally in the dc and rf mode.

Integrated over the entire rf-period, we calculated that for the rf mode, approximately 95% of the total amount of ionization of argon is due to electron impact (approx. 72% due to α-ionization and approximately 23% due to γ-ionization). The contributions of the fast argon atoms and argon ions were calculated to be 4% and 1%, respectively, which is of less importance, but not entirely negligible. Similar calculations were carried out for the dc case. It was found that approximately 89% of the ionization was due to electrons, and approximately 9% and 2% to fast argon atoms and argon ions, respectively. Hence, the fast argon ions and atoms in the dc-mode seem to have a slightly higher contribution in ionization than in the rf mode. This is attributed to two effects: (i) the higher dc voltage yields higher ion and atom energies and hence more efficient ionization; and (ii) in the rf mode electron impact ionization is relatively more important due to the large contribution of α-ionization around $\omega t = \pi/2$. Nevertheless, the overall trends in the relative contributions of electrons, argon ions and fast argon atoms are comparable in both the operation modes. This demonstrates again that for the rf-discharge conditions under considera-

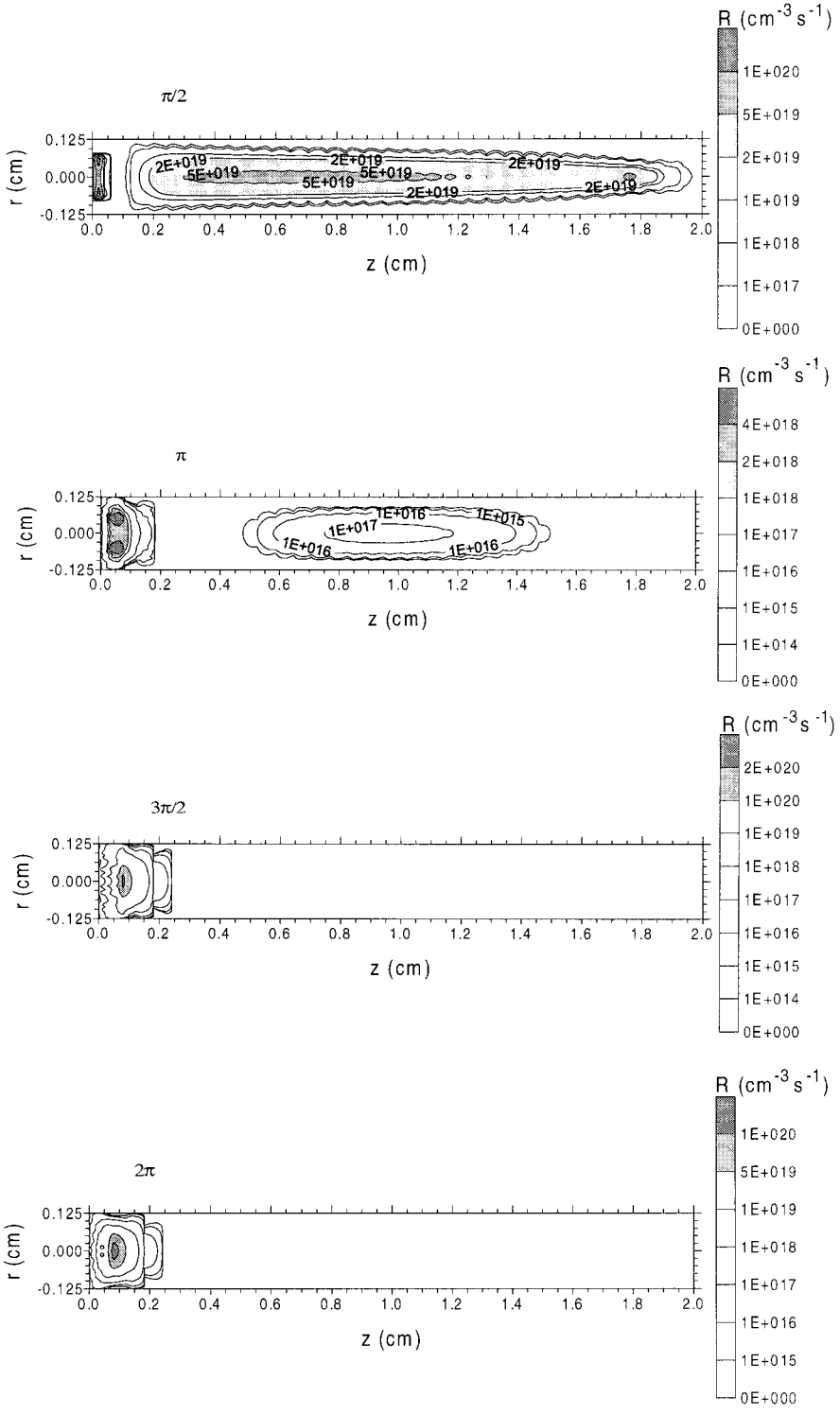

Fig. 10. Two-dimensional electron impact α-ionization rate of argon in the rf-discharge, throughout the discharge region at four times in the rf-cycle, calculated with the fluid model ($p = 5.775$ torr, $P = 10.2$ W).

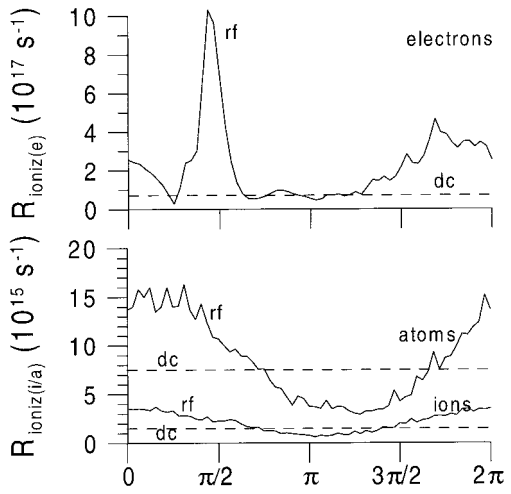

Fig. 11. Ionization rate of argon due to electron impact (upper part), and argon ion and atom impact (lower part of the figure), integrated over the entire discharge region, both calculated for the rf-mode (as a function of time in the rf-cycle; solid lines) and for the dc-mode (dashed lines) ($p = 5.775$ torr, $P = 10.2$ W rf and 10.45 W dc).

tion here, the rf-discharge resembles very much a dc discharge.

4. Conclusion

A hybrid Monte Carlo–fluid model has been developed for the electrons, argon ions and fast argon atoms in an argon glow discharge, operated either in the dc or in the rf mode. Typical results of this calculation comprise the electrical characteristics, the potential distribution, the electrical currents, the argon ion and slow electron densities, and the ionization rates in the plasma. The working conditions that have been simulated are typical for rf-GD-OES and were suggested by Hoffmann [8] because measured electrical characteristics (voltage, power, pressure) are available, i.e. 5.775 torr gas pressure, 1000 K gas temperature and 10.2 W electrical power. With these input data, an rf voltage of approximately 937 V and a dc bias voltage of -640 V were calculated. These calculated voltages are in reasonable agreement with experimental values [8]. Comparison has been made with a dc discharge at the same pressure, power and gas temperature. It was found that in the dc discharge a higher operating voltage (i.e. 1100 V) was needed to yield the same amount of power, compared to the corresponding dc bias voltage in the rf discharge. This demonstrates that ionization is more efficient in the rf-discharge than in the dc-discharge. The reason for this is that beside γ-ionization (i.e. due to electrons emitted from the rf-electrode or formed in the plasma with sufficient energy to cause ionization) also α-ionization occurs in the rf-mode. The latter mechanism is due to slow electrons in the bulk plasma which can become heated again due to the fluctuating rf electric field, and seems to be especially important around $\omega t = \pi/2$. Integrated over the entire rf-cycle and discharge region, we found that α and γ ionization contribute to the total ionization for approximately 72 and 23%, respectively (the remaining fraction is due to fast argon ion and atom impact ionization). Since in the dc mode only γ-ionization is possible, it becomes indeed clear that the rf mode will yield more efficient ionization than the dc mode. The difference in voltages between dc and rf modes, and hence also the difference in ionization efficiencies (which are directly related to it), are in excellent agreement with experimental observations [8].

Beside the ionization efficiency, also the argon ion and slow electron densities and the argon ion flux were found to be somewhat higher in the rf discharge than in the dc discharge. In future work, we plan to calculate also other glow discharge parameters, like sputtering rates, optical emission and ion intensities in the rf discharge, as we have done already for the dc discharge, in order to compare also these analytically more important parameters between both operation modes. These comparisons will then also be checked against experimental observations.

Apart from these differences in the absolute values, the relative profiles of the two-dimensional potential distributions, argon ion densities and ionization rates of argon calculated for the rf-discharge are, at least during the negative (i.e. the largest) part of the rf-cycle, more or less similar to the results for the dc-discharge. Hence, it can be concluded that, for the discharge condi-

tions under consideration, the rf-discharge resembles very much a dc-discharge, but with some extra possibility for ionization.

Acknowledgements

A. Bogaerts acknowledges financial support from the Flemish Fund for Scientific Research (FWO). This research is also sponsored by the Federal Services for Scientific, Technical and Cultural Affairs (DWTC/SSTC) of the Prime Minister's Office through IUAP-IV (Conv. P4/10). Finally we would like to thank V. Hoffmann for supplying the experimental data, and V. Hoffmann, K. Marcus, R. Payling, A. Bengtson, and Ph. Belenguer for the interesting and helpful discussions.

References

[1] R.K. Marcus, Glow Discharge Spectroscopies, Plenum Press, New York, 1993.
[2] R. Payling, D. Jones, A. Bengtson, Glow Discharge Optical Emission Spectrometry, Wiley, Chichester, 1997.
[3] X. Pan, B. Hu, Y. Y, R.K. Marcus, J. Anal. At. Spectrom. 13 (1998) 1159.
[4] C. Perez, R. Pereiro, N. Bordel, A. Sanz-Medel, Spectrochim. Acta 53B (1998) 1541.
[5] W.B. Cho, Y.A. Woo, H.J. Kim, I.J. Kim, W.K. Kang, Appl. Spectrosc. 51 (1997) 1060.
[6] F. Prässler, V. Hoffmann, J. Schumann, K. Wetzig, J. Anal. At. Spectrom. 10 (1995) 677.
[7] V. Hoffmann, H.-J. Uhlemann, F. Prässler, K. Wetzig, D. Birus, Fresenius J. Anal. Chem. 355 (1996) 826.
[8] V. Hoffmann, unpublished results.
[9] S. De Gendt, R. Van Grieken, W. Hang, W.W. Harrison, J. Anal. At. Spectrom. 10 (1995) 689.
[10] D. Pollmann, K. Ingeneri, W.W. Harrison, J. Anal. At. Spectrom. 11 (1996) 849.
[11] R. Payling, D.G. Jones, S.A. Gower, Surf. Interface Anal. 20 (1993) 959.
[12] K. Wagatsuma, S. Suzuki, Fresenius J. Anal. Chem. 358 (1997) 581.
[13] R. Payling, private communication.
[14] A. Bogaerts, R. Gijbels, W. Goedheer, J. Appl. Phys. 78 (1995) 2233.
[15] A. Bogaerts, R. Gijbels, W. Goedheer, Anal. Chem. 68 (1996) 2296.
[16] A. Bogaerts, R. Gijbels, J. Appl. Phys. 78 (1995) 6427.
[17] A. Bogaerts, R. Gijbels, W. Goedheer, Jpn. J. Appl. Phys. 38 (1999).
[18] A. Bogaerts, R. Gijbels, IEEE Trans. Plasma Sci. (1999) in press.
[19] A. Bogaerts, M. Yan, R. Gijbels, W. Goedheer, J. Appl. Phys. (1999) in press.
[20] N.P. Ferreira, H.G.C. Human, L.R.P. Butler, Spectrochim. Acta 35B (1980) 287.
[21] A.V. Phelps, Z. Lj. Petrovic, Plasma Sources Sci. Technol. (submitted); also: http://jilaweb.colorado.edu/www/research/colldata.html
[22] S. Hashiguchi, IEEE Trans. Plasma Sci. 19 (1991) 297.
[23] A.V. Phelps, J. Phys. Chem. Ref. Data 20 (1991) 557.
[24] A.V. Phelps, J. Appl. Phys. 76 (1994) 747.
[25] H. Oechsner, Phys. Rev. B 17 (1978) 1052.
[26] A. Bogaerts, M. van Straaten, R. Gijbels, Spectrochim. Acta 50B (1995) 179.
[27] B. Chapman, Glow Discharge Processes, Wiley, New York, 1980.
[28] M.J. Kushner, IEEE Trans. Plasma Sci. PS 13 (1986) 112.
[29] Ph. Belenguer, J.P. Boeuf, Phys. Rev. A 41 (1990) 4447.
[30] M. Surendra, D.B. Graves, IEEE Trans. Plasma Sci. PS 19 (1991) 144.
[31] F.W. Aston, Proc. R. Soc. London Ser. A 79 (1907) 80.
[32] D.B. Graves, K.F. Jensen, IEEE Trans. Plasma Sci. 14 (1986) 78.
[33] D. Passchier, Ph.D. Thesis, University of Utrecht (1994).